Atmos. Chem. Phys. Discuss., doi:10.5194/acp-2016-1189, 2017
Manuscript under review for journal Atmos. Chem. Phys.
Published: 2 February 2017

Atmospheric Chemistry and Physics
Discussions

Multi-model ensemble simulations of olive pollen distribution in Europe in 2014.

Mikhail Sofiev[1], Olga Ritenberga[2], Roberto Albertini[3], Joaquim Arteta[4], Jordina Belmonte[5,6], Maira Bonini[7], Sevcan Celenk[8], Athanasios Damialis[9,10], John Douros[11], Hendrik Elbern[12], Elmar Friese[12], Carmen Galan[13], Oliver Gilles[14], Ivana Hrga[15], Rostislav Kouznetsov[1], Kai Krajsek[16], Jonathan Parmentier[4], Matthieu Plu[4], Marje Prank[1], Lennart Robertson[17], Birthe Marie Steensen[18], Michel Thibaudon[14], Arjo Segers[19], Barbara Stepanovich[15], Alvaro M. Valdebenito[18], Julius Vira[1], Despoina Vokou[10]

[1] Finnish Meteorological Institute, Erik Palmenin Aukio 1, Finland
[2] University of Latvia, Latvia
[3] Department of Clinical and Experimental Medicine, University of Parma, Italy
[4] CNRM UMR 3589, Météo-France/CNRS, Toulouse, France
[5] Institute of Environmental Sciences and Technology (ICTA), Universitat Autònoma de Barcelona, Spain
[6] Depatment of Animal Biology, Plant Biology and Ecology, Universitat Autònoma de Barcelona, Spain
[7] Agenzia Tutela della Salute della Città Metropolitana di Milano/ LHA ATS Città Metropolitana Milano, Italy
[8] Biology department, Uludag University, Turkey
[9] Chair and Institute of Environmental Medicine, UNIKA-T, Technical University of Munich and Helmholtz Zentrum München - German Research Center for Environmental Health, Augsburg, Germany
[10] Department of Ecology, School of Biology, Aristotle University of Thessaloniki, Greece
[11] Royal Netherlands Meteorological Institute, De Bilt, The Netherlands
[12] Rhenish Institute for Environmental Research at the University of Cologne, Germany
[13] University of Cordoba, Spain
[14] RNSA, Brussieu, France
[15] Andrija Stampar Teaching Institute of Public Health, Croatia
[16] Institute of Energy and Climate Research (IEK-8), Forschungszentrum Jülich, Germany
[17] Swedish Meteorological and Hydrological Institute SMHI, Sweden
[18] MET Norway
[19] TNO, Netherlands

1. Abstract

A 6-models strong European ensemble of Copernicus Atmospheric Monitoring Service (CAMS) was run through the season of 2014 computing the olive pollen dispersion in Europe. The simulations have been compared with observations in 6 countries, members of the European Aeroallergen Network. Analysis was performed for individual models, the ensemble mean and

Atmos. Chem. Phys. Discuss., doi:10.5194/acp-2016-1189, 2017
Manuscript under review for journal Atmos. Chem. Phys.
Published: 2 February 2017

median, and for a dynamically optimized combination of the ensemble members obtained via fusion of the model predictions with observations. The models, generally reproducing the olive season of 2014, showed noticeable deviations from both observations and each other. In particular, the season start was reported too early, by 8 days but for some models the error mounted to almost two weeks. For the season end, the disagreement between the models and the observations varied from a nearly perfect match up to two weeks too late. A series of sensitivity studies performed to understand the origin of the disagreements revealed crucial role of ambient temperature, especially systematic biases in its representation by meteorological models. A simple correction to the heat sum threshold eliminated the season shift but its validity in other years remains to be checked. The short-term features of the concentration time series were reproduced better suggesting that the precipitation events and cold/warm spells, as well as the large-scale transport were represented rather well. Ensemble averaging led to more robust results. The best skill scores were obtained with data fusion, which used the previous-days observations to identify the optimal weighting coefficients of the individual model forecasts. Such combinations were tested for the forecasting period up to 4 days and shown to remain nearly optimal throughout the whole period.

Keywords: olive pollen, airborne pollen modelling, pollen forecasting, multi-model ensemble, data fusion, aerobiology

2. Introduction

Biogenic aerosols, such as pollen and spores, constitute a substantial fraction of particulate matter mass in the air during the vegetation flowering season and can have strong health effects causing allergenic rhinitis and asthma (G D'Amato et al., 2007). One of important allergenic trees is olive.

Olive is one of the most extensive crops and its oil being one of the major economic resources in Southern Europe. The bulk of olive habitation (95% of the total area worldwide) is concentrated in the Mediterranean basin (Barranco et al., 2008). Andalusia has by far the world's largest area given over to olive plantations, 62% of the total olive land of Spain and 15% of the world's plantations (Gómez et al., 2014).

Olive pollen is also one of the most important causes of respiratory allergies in the Mediterranean basin (G. D'Amato et al., 2007) and in Andalusia it is considered as the main cause of allergy. In Cordoba City (S Spain), 73% of pollen-allergy sufferers are sensitive to olive pollen (Sánchez-Mesa et al., 2005). High rates of sensitization to olive pollen have been documented in many other Mediterranean countries: 31.8% in Greece (Gioulekas et al., 2004), 27.5% in Portugal (Loureiro et al., 2005), 24% in Italy (Negrini et al., 1992), 21.6% in Turkey (Kalyoncu et al., 1995), and 15% in France (Spieksma, 1990).

Olive is an entomophilous species that presents a secondary anemophily, favored by the agricultural management during the last centuries. This tree is very well adapted to the Mediterranean climate and tolerates the high summer and the low winter temperatures, as well as the summer drought, characteristic for this climate.

Olive floral phenology is characterized by bud formation during summer, dormancy during autumn, budburst in late winter, and flowering in late spring (Fernandez-Escobar et al., 1992; Galán et al., 2005; García-mozo et al., 2006). Similar to some other trees, olive flowering intensity shows alternated years with high and low or even no pollen production. The characteristic quasi-biannual cycles are well visible in observations (Ben Dhiab et al., 2016; Garcia-Mozo et al., 2014). This cycle, similar to other trees, e.g., birch, is not strict and is frequently interrupted showing several years with similar flowering intensity (Garcia-Mozo et al., 2014). Such cyclic behavior is related to the reproductive development, which is completed in two consecutive years. In the first year, the bud vegetative or reproductive character is determined by the current harvest level, since this is the main factor responsible for the inter-annual variation of flowering. In the second year, after the winter rest, the potentially reproductive buds that have fulfilled their chilling requirements develop into inflorescences (Barranco et al., 2008).

After the bud break, certain bio-thermic units are required for the development of the inflorescences. Both the onset of the heat accumulation period and the temperature threshold for the amount of positive heat units might vary according to the climate of a determined geographical area. The threshold level was also reported to decrease towards the north (Aguilera et al., 2013). Altitude is the topographical factor most influencing olive local phenology and the major weather factors are temperature, rainfall, and solar radiation that control the plant evapotranspiration (Oteros et al., 2013; Oteros et al., 2014).

Several studies used airborne pollen as a predictor variable for determining the potential sources of olive pollen emission, e.g. Concentric Ring Method (Oteros et al., 2015), geostatistical techniques (Rojo and Pérez-Badia, 2015) and the spatio-temporal airborne pollen maps (Aguilera et al., 2015).

There is a substantial variability of olive biological characteristics and its responses to environmental stresses. In particular, the allergen content was shown to be strongly different in pollen coming from different parts of the Iberian Peninsula (Galan et al., 2013).

Atmos. Chem. Phys. Discuss., doi:10.5194/acp-2016-1189, 2017
Manuscript under review for journal Atmos. Chem. Phys.
Published: 2 February 2017

Atmospheric Chemistry and Physics Discussions

Numerical modelling of olive pollen transport is very limited. In fact, the only regional-scale computations regularly performed since 2008 were made by the SILAM model (http://silam.fmi.fi) but the methodology was only scarcely outlined in (Galan et al., 2013).

Copernicus Atmospheric Monitoring Service CAMS (http://atmosphere.copernicus.eu) is one of the services of the EU Copernicus program, addressing various global and regional aspects of atmospheric state and composition. CAMS European air quality ensemble (Marécal et al., 2015) provides high-resolution forecasts and reanalysis of the atmospheric composition over Europe. Olive pollen is one of the components, which are being introduced in the CAMS European ensemble in co-operation with European Aeroallergen Network EAN (https://www.polleninfo.org/country-choose.html).

One of possible ways of improving the quality of model predictions without direct application of data assimilation is to combine them with observations via ensemble-based data fusion methods (Potempski and Galmarini, 2009). Their efficiency has been demonstrated for air quality problems (Johansson et al., 2015 and references therein) and climatological models (Genikhovich et al., 2010) but the technology has never been applied to pollen.

The aim of the current publication is to present the first Europe-wide ensemble-based evaluation of the olive pollen dispersion during the season of 2014. The study followed the approach of the multi-model simulations for birch (Sofiev et al., 2015) with several amendments reflecting the peculiarity of olive pollen distribution in Europe. We also made further steps towards fusion of model predictions and observations and demonstrate its value in the forecasting regime.

The next section will present the participating models and setup of the simulations, the observation data used for evaluation of the model predictions, approach for constructing an optimised multi-model ensemble, and a list of sensitivity computations. The Results section will present the outcome of the simulations and the quality scores of the individual models and the ensemble. The Discussion section will be dedicated to analysis of the results, considerations of the efficiency of the multi-model ensemble for olive pollen, and identification of the development needs.

3. Materials and methods

This section presents the regional models used in the study, outlines the olive pollen source term implemented in all of them, and pollen observations used for evaluation of the model predictions.

Atmos. Chem. Phys. Discuss., doi:10.5194/acp-2016-1189, 2017
Manuscript under review for journal Atmos. Chem. Phys.
Published: 2 February 2017

3.1. Dispersion models

The dispersion models used in the study comprise the CAMS European ensemble, which is described in details by Marécal et al., (2015) and (Sofiev et al., 2015). Below, only the model features relevant for the olive pollen atmospheric transport calculations are described.

The ensemble consisted of six models.

EMEP model of EMEP/MSC-West (European Monitoring and Evaluation Programme / Meteorological Synthesizing Centre - West) is a chemical transport model developed at the Norwegian Meteorological Institute and described in Simpson et al., (2012). It is flexible with respect to the choice of projection and grid resolution. Dry deposition is handled in the lowest model layer. A resistance analogy formulation is used to describe dry deposition of gases, whereas for aerosols the mass-conservative equation is adopted from Venkatram, (1978) with the dry deposition velocities dependent on the land use type. Wet scavenging is dependent on precipitation intensity and is treated differently within and below cloud. The below-cloud scavenging rates for particles are based on Scott, (1979). The rates are size-dependent, growing for larger particles.

EURAD-IM (http://www.eurad.uni-koeln.de) is an Eulerian meso-scale chemistry transport model involving advection, diffusion, chemical transformation, wet and dry deposition and sedimentation of tropospheric trace gases and aerosols (Hass et al., 1995; Memmesheimer et al., 2004). It includes 3D-VAR and 4D-VAR chemical data assimilation (Elbern et al., 2007) and is able to run in nesting mode. The positive definite advection scheme of Bott (1989) is used to solve the advective transport and the aerosol sedimentation. An eddy diffusion approach is applied to parameterize the vertical sub-grid-scale turbulent transport (Holtslag and Nieuwstadt, 1986). Dry deposition of aerosol species is treated size-dependent using the resistance model of Petroff and Zhang (2010). Wet deposition of pollen is parameterized according to Baklanov and Sorensen (2001).

LOTOS-EUROS (http://www.lotos-euros.nl/) is an Eulerian chemical transport model (Schaap et al., 2008). The advection scheme follows Walcek and Aleksic (1998). The dry deposition scheme of Zhang et al. (2001) is used to describe the surface uptake of aerosols. Below-cloud scavenging is described using simple scavenging coefficients for particles (Simpson et al., 2003).

MATCH (http://www.smhi.se/en/research/research-departments/air-quality/match-transport-and-chemistry-model-1.6831) is an Eulerian multi-scale chemical transport model with mass-conservative transport and diffusion based on a Bott-type advection scheme (Langner et al., 1998; Robertson and Langner, 1999). For olive pollen, dry deposition is mainly treated by sedimentation

Atmos. Chem. Phys. Discuss., doi:10.5194/acp-2016-1189, 2017
Manuscript under review for journal Atmos. Chem. Phys.
Published: 2 February 2017

and a simplified wet scavenging scheme is applied. The temperature sum, which drives pollen emission, is computed off-line starting from January onwards and is fed into the emission module.

MOCAGE (http://www.cnrm.meteo.fr/gmgec-old/site_engl/mocage/mocage_en.html) is a multi-scale dispersion model with grid-nesting capability (Josse et al., 2004; Martet et al., 2009). The semi-Lagrangian advection scheme of Williamson and Rasch (1989) is used for the grid-scale transport. The convective transport is based on the parameterization proposed by Bechtold et al. (2001) whereas the turbulent diffusion follows the parameterization of Louis (1979). Dry deposition including the sedimentation scheme follows Seinfeld and Pandis (1998). The wet deposition by the convective and stratiform precipitations is based on Giorgi and Chameides (1986).

SILAM (http://silam.fmi.fi) is a meso-to-global scale dispersion model (Sofiev et al., 2015), also described in the review of Kukkonen et al. (2012). Its dry deposition scheme (Kouznetsov and Sofiev, 2012) is applicable for a wide range of particle sizes including coarse aerosols, which are primarily removed by sedimentation. The wet deposition parameterization distinguishes between sub- and in-cloud scavenging by both rain and snow (Sofiev et al., 2006). For coarse particles, impaction scavenging parameterised following (Kouznetsov and Sofiev, 2012) is dominant below the cloud. The model includes emission modules for six pollen types: birch, olive, grass, ragweed, mugwort, and alder, albeit only birch, ragweed, and grass sources are so-far described in the literature (Prank et al., 2013; Sofiev, 2016; Sofiev et al., 2012).

Three **ENSEMBLE** models were generated by (i) arithmetic average, (ii) median and (iii) optimal combination of the 6 model fields. Averaging and median were taken on hourly basis, whereas optimization was applied at daily level following the temporal resolution of the observational data. For the current work, we used simple linear combination c_{opt} of the models c_m, $m=1..M$ minimising the regularised RMSE J of the optimal field:

(1) $$c_{opt}(i,j,k,t,A) = a_0(t) + \sum_{m=1}^{M} a_m(t)\, c_m(i,j,k,t), \quad A=[a_1..a_M], \quad a_m \geq 0\ \forall m$$

(2) $$J(\tau) = sqrt\left[\frac{1}{O}\sum_{o=1}^{O}\left(c_{opt}(i_o,j_o,k_o,\tau,A) - c_o(t)\right)^2\right] + \alpha\sum_{m=1}^{M}\left(a_m(\tau) - \frac{1}{M}\right)^2 + \beta\sum_{m=1}^{M}\left(a_m(\tau-1) - a_m(\tau)\right)^2, \qquad \tau = \{d_{-k}, d_0\}$$

Here, i,j,k,t are indices along the x,y,z, and time axes, M is the number of models in the ensemble, O is the number of observation stations, $\tau = \{d_{-k}:d_0\}$ is the time period of $k+1$ days covered by the analysis window, starting from d_{-k} until d_0 , τ -1 is the previous-day analysis period $\tau -1=\{d_{-k-1}:d_{-1}\}$,

Atmos. Chem. Phys. Discuss., doi:10.5194/acp-2016-1189, 2017
Manuscript under review for journal Atmos. Chem. Phys.
Published: 2 February 2017

c_m is concentration of pollen predicted by the model m, a_m is time-dependent weight coefficient of the model m in the ensemble. In the Eq. (2), the first term represents the RMSE of the assimilated period τ, the second term limits the departure of the coefficients from the homogeneous weight distribution, the third one limits the speed of evolution of the a_m coefficients in time. The scaling values α and β decide on the strength of regularization imposed by these two terms.

The ensemble was constructed mimicking the forecasting mode. Firstly, the analysis is made using data from the analysis period τ . The obtained weighting coefficients a_i are used over several days forwards from day d_0: from d_1 until d_{nf}, which constitute the forecasting steps. The performance of the ensemble is evaluated for each length of the forecast, from *1* to n_f days.

3.2. Olive pollen source term

All models of this study are equipped with the same olive pollen source term, which has not been described in the scientific literature yet. However, it follows the same concept as the birch source (Sofiev et al., 2012) that was used for the birch ensemble simulations (Sofiev et al., 2015). The formulations and input data are open at http://silam.fmi.fi/MACC. The main input dataset is the annual olive pollen production map based on ECOCLIMAP dataset (Champeaux et al., 2005; Masson et al., 2003), Figure 1.

ECOCLIMAP incorporates the CORINE land-cover data for most of western-European countries with explicit olive-plantations land-use type (CEC, 1993). For Africa and countries missing from CORINE, the empty areas were filled manually assuming that 10% of all tree-like land-use types are olives. This way, Tunisian, Egyptian, and Algerian olive plantations were recovered and included in the inventory. In some areas, such as France (Figure 1), the olive habitat looks unrealistically low, probably because the large olive plantations are rare but the trees are planted in private gardens, city park areas, streets, etc. Since these distributed sources are not reflected in the existing land-use inventories, they are not included in the current pollen production map.

Similar to birch, the flowering description follows the concept of Thermal Time phenological models and, in particular, the double-threshold air temperature sum approach of Linkosalo et al. (2010) modified by Sofiev et al. (2012). Within that approach, the heat accumulation starts on a prescribed day in spring (1 January in the current setup – after Spano et al. (1999), Moriondo et al. (2001), Orlandi et al. (2005a, 2005b) and continues throughout spring. The cut-off daily temperature below which no summation occurs is 0°C, as compares to 3.5°C for birch, was obtained from the multi-annual fitting of the season start. Flowering starts when the accumulated heat reaches the starting threshold (Figure 2) and continues until the heat reaches the ending threshold (in the current setup, equal to the start-season threshold + 275 degree day). The rate of heat accumulation is the main controlling parameter for pollen emission: the model assumes direct proportionality between the flowering stage and fraction of the heat sum accumulated to-date.

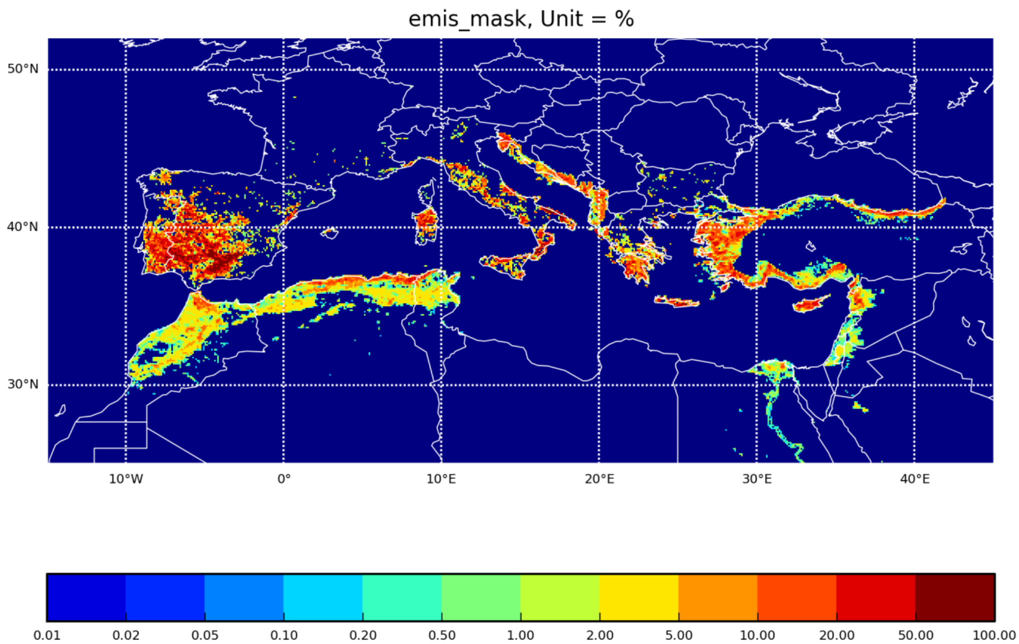

Figure 1. Olive pollen habitat map, percentage of the area occupied by the trees, [%]. Productivity of an area with 100% olive coverage is assumed to be 10^{10} pollen grain m^{-2} $season^{-1}$.

Similar to birch parameterization of Sofiev et al. (2012), the model distinguishes between the pollen maturation, which is solely controlled by the heat accumulation described above, and pollen release, which depends on other parameters. Higher relative humidity (RH) and rain reduce the release, completely stopping it for RH > 80% and/or rain > 0.1 mm hr^{-1}. Strong wind promotes it by up to 50%. Atmospheric turbulence is taken into account via the turbulent velocity scale and thus becomes important only in cases close to free convection. In stable or neutral stratification and calm conditions the release is suppressed by 50%. The interplay between the pollen maturation and release is controlled by an intermediate ready-pollen buffer, which is filled-in by the maturation and emptied by the release flows.

Local-scale variability of flowering requires probabilistic description of its propagation (Siljamo et al., 2008). In the simplest form, the probability of an individual tree entering the flowering stage can be considered via the uncertainty of the temperature sum threshold determining the start of flowering for the grid cell – 10% in the current simulations. The end of the season is described via the open-pocket principle: the flowering continues until the initially available amount of pollen is completely released. The uncertainty of this number is taken to be 10% as well.

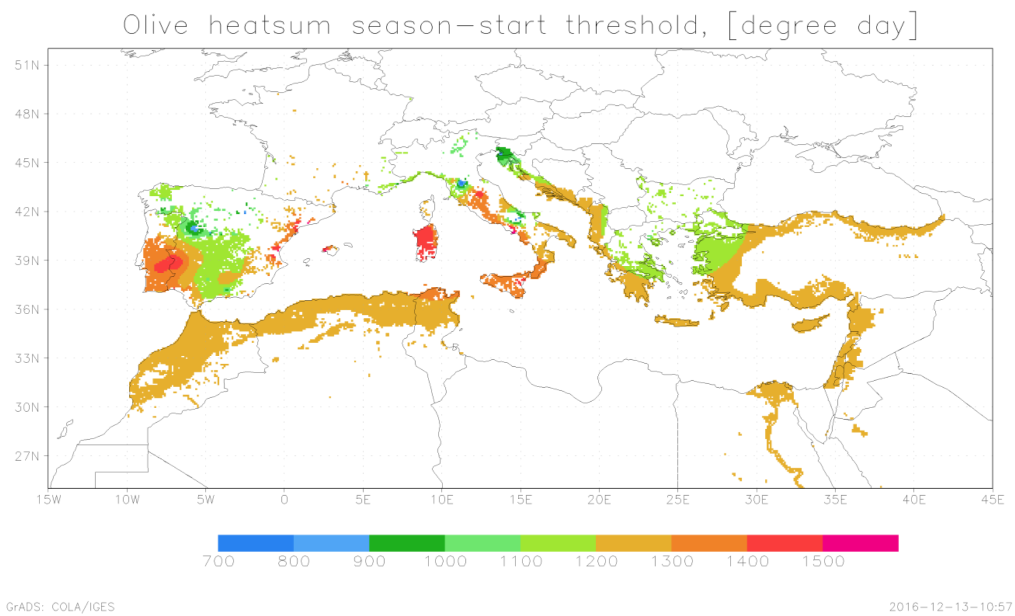

Figure 2. Heat sum threshold for the start of the season. Unit = [degree day]

3.3. Pollen observations

The observations for the model evaluation in 2014 have been provided by the following 6 national networks, members of the European Aeroallergen Network (EAN): Croatia, Greece, France, Italy, Spain, Turkey. The data were screened for completeness and existence of non-negligible olive season: (i) time series should have at least 30 valid observations, (ii) at least 10 daily values during the season should exceed 3 pollen m^{-3}, and (iii) the seasonal pollen index should be at least 25 pollen day m^{-3}. After this screening, information of 60 sites was used in the intercomparison.

Atmos. Chem. Phys. Discuss., doi:10.5194/acp-2016-1189, 2017
Manuscript under review for journal Atmos. Chem. Phys.
Published: 2 February 2017

Pollen monitoring was performed with Burkard 7-day and Lanzoni 2000 pollen traps based on the Hirst design (Hirst, 1952). The pollen grains were collected at an airflow rate of 10 l min^{-1}. The observations covered the period from March until September, with some variations between the countries. Daily pollen concentrations were used. Following the EAS-EAN requirements (Galán et al., 2014; Jäger et al., 1995), most samplers were located at heights of between 10m and 30m on the roofs of suitable buildings. The places were frequently downtown of the cities, i.e. largely represent the urban-background conditions (not always though). With regard to microscopic analysis, the EAS-EAN requirements is to count at least 10% of the sample using horizontal or vertical strips (Galán et al., 2014). The actual procedures vary between the countries but generally comply. The counting in 2014 was mainly performed along four horizontal traverses as suggested by Mandrioli et al., (1998). In all cases, the data were expressed as mean daily concentrations (pollen m^{-3}).

3.4. Setup of the simulations

Simulations followed the standards of CAMS European ensemble (Marécal et al., 2015). The domain spanned from 25°W to 45°E and from 30°N to 70°N. Each of the 6 models was run with its own horizontal and vertical resolutions, which varied from 0.1° to 0.25° of the horizontal grid cell size, and had from 3 up to 52 vertical layers within the troposphere (Table 1). This range of resolutions is not designed to reproduce local aspects of pollen distribution, instead covering the whole continent and describing the large-scale transport events. The 10km grid cells reach the sub-city scale but still insufficient to resolve the valleys and individual mountain ridges. The limited number of vertical dispersion layers used by some models is a compromise allowing for high horizontal resolution. Thick layers are not a major limitation as long as the full vertical resolution of the input meteorological data is used for evaluation of dispersion parameters (Sofiev, 2002).

The simulations were made retrospectively for the season of 2014 starting from 1 January (the beginning of the heat sum accumulation) until 30 June when the pollen season was over. All models produced hourly output maps with concentrations at 8 vertical levels (near surface, 50, 250, 500, 1000, 2000, 3000 and 5000 metres above the surface), as well as dry and wet deposition maps.

All models considered pollen as an inert water-insoluble particle 28 μm in diameter and with a density of 800 kg m^{-3}.

Atmos. Chem. Phys. Discuss., doi:10.5194/acp-2016-1189, 2017
Manuscript under review for journal Atmos. Chem. Phys.
Published: 2 February 2017

Atmospheric Chemistry and Physics Discussions
Open Access

Table 1. Setup of the simulations for the participating models

Model	Horizontal dispersion grid	Dispersion vertical	Meteo input	Meteo grid	Meteo vertical
EMEP	0.25° × 0.125°	20 levels up to 100 hPa	ECMWF IFS 00 operational forecast, internal preprocessor	0.25° × 0.125°	IFS lvs 39 – 91 up to 100 hPa
EURAD-IM	15 km, Lambert conformal proj.	23 layers up to 100 hPa	WRF based on ECMWF IFS	Same as CTM	Same as CTM
LOTOS-EUROS	0.25° × 0.125°	3 dyn. lyrs up to 3.5km, sfc 25m	ECMWF IFS 00 operational forecast, internal preprocessor	0.5° × 0.25°	IFS lvs 69-91 up to 3.5km
MATCH	0.2° × 0.2°	52 layers up to 7 km	ECMWF IFS 00 from MARS, internal preprocessor	0.2° × 0.2°	IFS vertical: 91 lvs
MOCAGE	0.2° x 0.2°	47 layers up to 5hPa (7 in ABL)	ECMWF IFS 00 operational forecast, internal preprocessor	0.125° × 0.125°	IFS vertical 91 lvs
SILAM	0.1° × 0.1°	9 layers up to 7.5 km	ECMWF IFS 00 operational forecast, internal preprocessor	0.125° × 0.125°	IFS lvs 62-137 up to ~110hPa

4. Results for the pollen season of 2014

4.1. Observed peculiarities of the season

At French Mediterranean stations (Aix-en-Provence, Avignon, Montpellier, Nice, Nîmes and Toulon), the mean value of 2014 Seasonal Pollen Index (SPI) for olive tree was quite similar to that of 2012 but lower than in 2013. The start of the pollen season was earlier than in the previous five years. The duration of the season has been the longest one on Aix-en-Provence, Nice and Nîmes since 2010. On Ajaccio (Corsica) station, the SPI was higher in 2014 than at other stations, similar to the situation in 2012.

In Andalusia, 2014 was the second warmest year during the last decades but more humid than usual, 5% above the typical relative humidity level (https://www.ncdc.noaa.gov/sotc/global/201413). However, after an intense olive flowering in 2013, in 2014 the flowering intensity was lower and similar to 2012, in agreement with the bi-annual alterations of the season severity.

In Northern Italy, the 2014 olive pollen season was less intense than the average of the previous ten years (2004-2013). Instead, in Southern Italy, the 2014 season was more intense in the first part and less intense in the second part (after the beginning of June) than during previous seasons. No differences were noted respect the start and the end of the season in both cases.

Atmos. Chem. Phys. Discuss., doi:10.5194/acp-2016-1189, 2017
Manuscript under review for journal Atmos. Chem. Phys.
Published: 2 February 2017

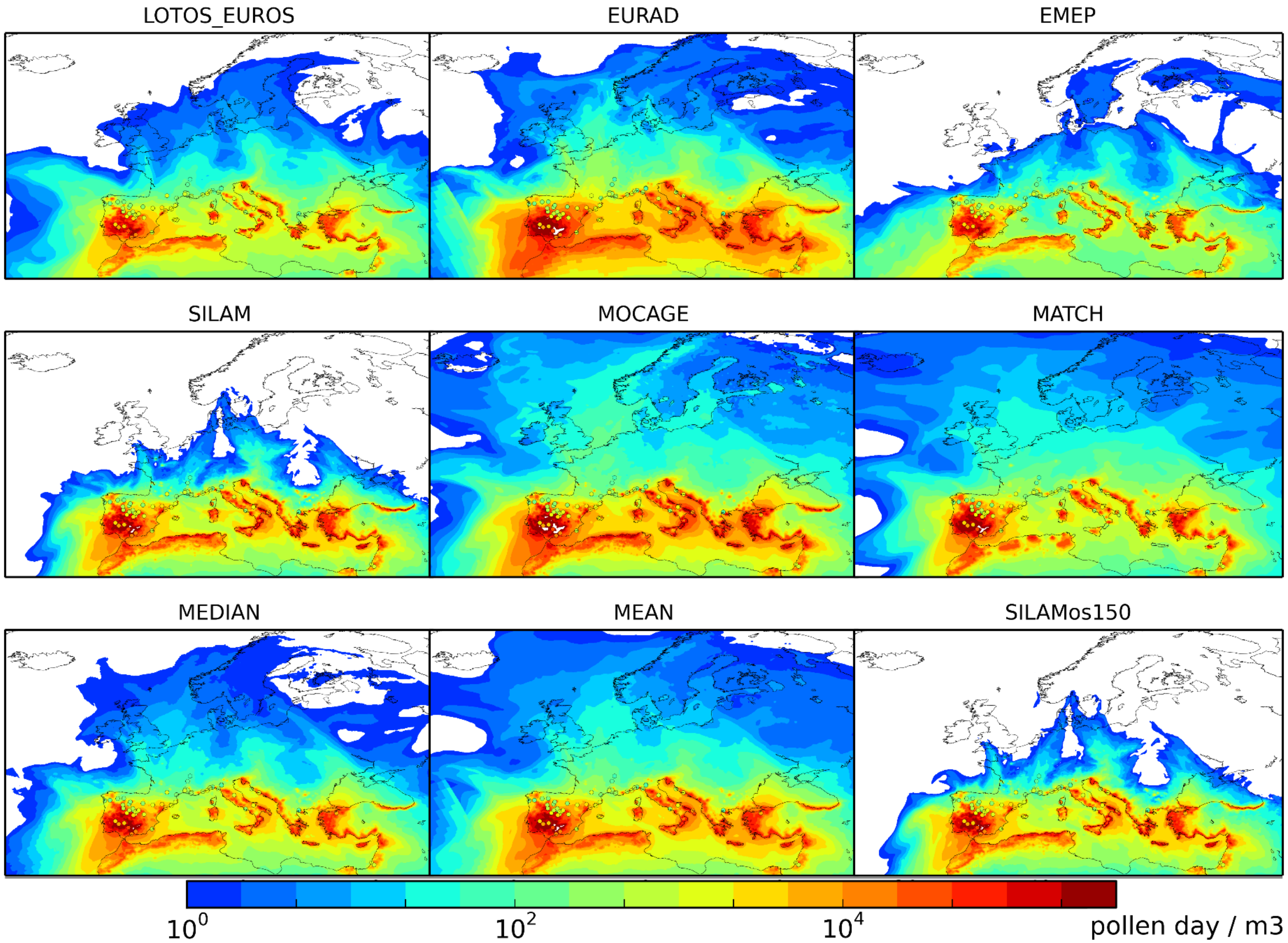

Figure 3. Observed (dots) and modelled (shades) Seasonal Pollen Index (SPI, sum of daily concentrations), 2014, [pollen day m^{-3}].

Atmos. Chem. Phys. Discuss., doi:10.5194/acp-2016-1189, 2017
Manuscript under review for journal Atmos. Chem. Phys.
Published: 2 February 2017

Atmospheric Chemistry and Physics
Discussions

4.2. Model results

The total seasonal olive pollen load (Figure 3) expectedly correlates with the map of olive plantations (Figure 1), which is also confirmed by the observations (Figure 3). The highest load is predicted over Spain and Portugal, whereas the level in the Eastern Mediterranean is not so high reflecting smaller size of the areas covered by the olive trees. The model predictions differ up to a factor of a few times, reflecting the diversity of modelling approaches, especially the deposition and vertical diffusion parameterizations (see Table 1 and section 3.1).

Since the olive plantations are located within a comparatively narrow climatic range, flowering propagates through the whole region within a few weeks starting from the coastal bands and progressing inland (not shown).

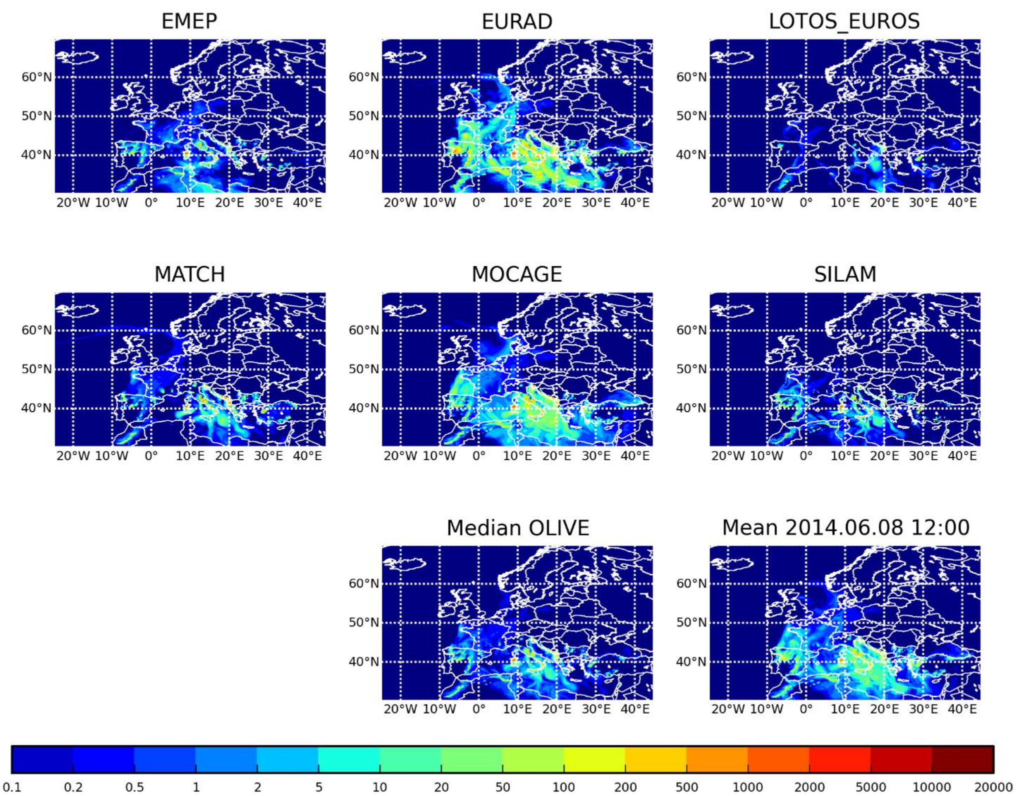

Figure 4. Example of hourly olive pollen concentrations, 12 UTC 08.06.2014, [pollen m^{-3}].

Atmos. Chem. Phys. Discuss., doi:10.5194/acp-2016-1189, 2017
Manuscript under review for journal Atmos. Chem. Phys.
Published: 2 February 2017

Atmospheric Chemistry and Physics Discussions

Hot weather during the flowering season leads to strong vertical mixing and deep atmospheric boundary layer (ABL), which in turn promotes the pollen dispersion. As seen from Figure 4, the pollen plumes can reach out over the whole Mediterranean and episodically affect Central Europe. Both Figure 3 and Figure 4 illustrate the differences between the models, e.g. substantially higher concentrations reported by EURAD-IM and MOCAGE as compared to other models. What regard to pollen transport, the shortest transport with the fastest deposition is manifested by LOTOS-EUROS (also, showed the lowest concentrations), while the longest one is suggested by MOCAGE.

The most-important general parameters describing the season timing are its start and end (Figure 5). Following Andersen (1991), these dates are computed as dates when 5% and 95% of the SPI are reached.

Computations of the model-measurement comparison statistics faces the problem of non-stationarity and non-normal distribution of the daily pollen concentrations (Ritenberga et al., 2016). For such processes, usual non-parametric statistics have to be taken with high care since their basic assumptions are violated. Nevertheless, they can be formally calculated for both individual models and the ensemble (Figure 6, Figure 7). The main characteristic of the ensemble, the discrete rank histogram and the distribution of the modelled values for the below-detection-limit observations (Figure 8) show that the spread of the obtained ensemble is somewhat too narrow in comparison with the dynamic range of the observations. The same limitation was noticed for the birch ensemble.

The patterns in Figure 5 and Figure 6 reveal a systematic early bias of the predicted season start and end, which is well seen from normalised cumulative concentration time series (Figure 9). This bias is nearly identical for all models, except for EURAD-IM, which also shows higher correlation coefficient than other models. The reasons for the problem and for the diversity of the model response are discussed in the next section.

Atmos. Chem. Phys. Discuss., doi:10.5194/acp-2016-1189, 2017
Manuscript under review for journal Atmos. Chem. Phys.
Published: 2 February 2017

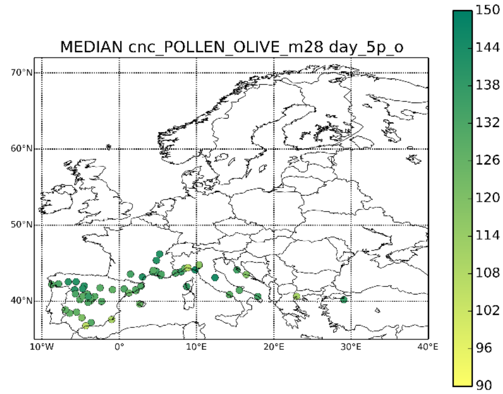

Season start day, 5%, observed

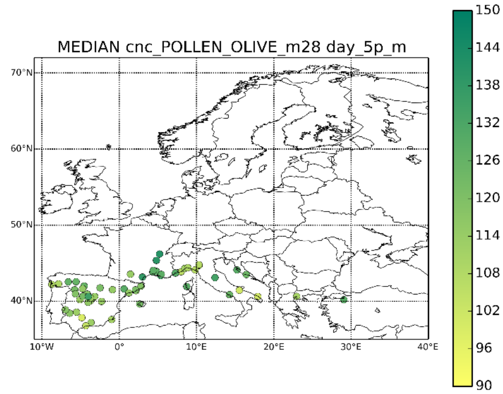

Season start day, 5%, ensemble median

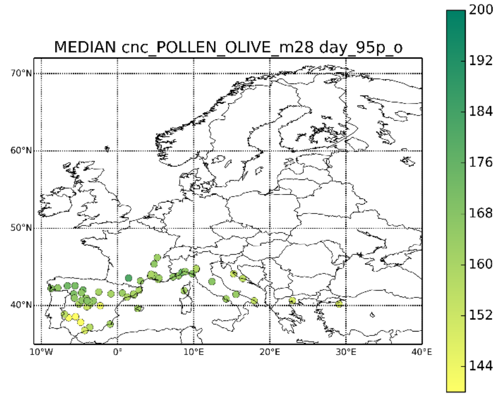

Season end day, 95%, observed

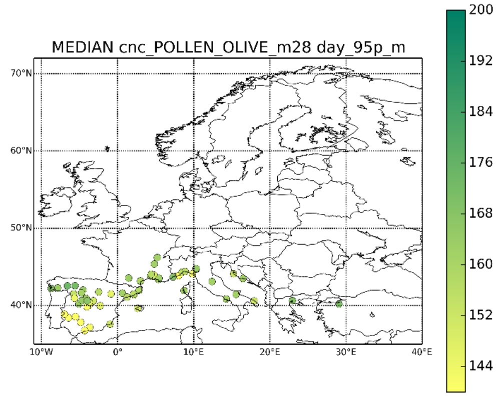

Season end day, 95%, ensemble median

Figure 5. The start (date of 5% of the cumulative seasonal concentrations) and the end (95% of the cumulative seasonal concentrations) of the olive season in 2014 as day of the year, predicted by the median of the ensemble and observed by the stations with sufficient amount of observations.

Atmos. Chem. Phys. Discuss., doi:10.5194/acp-2016-1189, 2017
Manuscript under review for journal Atmos. Chem. Phys.
Published: 2 February 2017

Atmospheric Chemistry and Physics
Open Access
EGU
Discussions

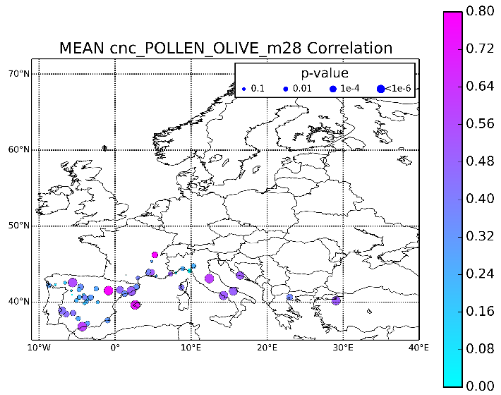

Correlation coefficient, dot size refers to p-value

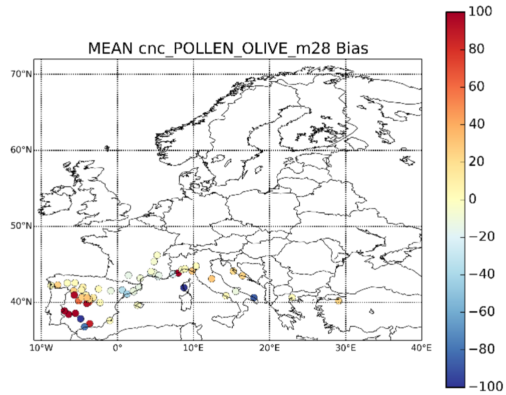

Absolute bias, mean April-June, [pollen m^{-3}]

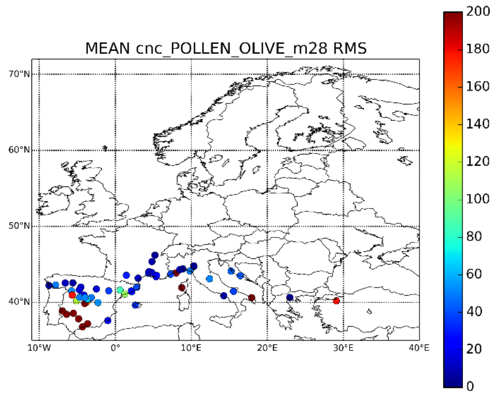

RMSE, [pollen m^{-3}]

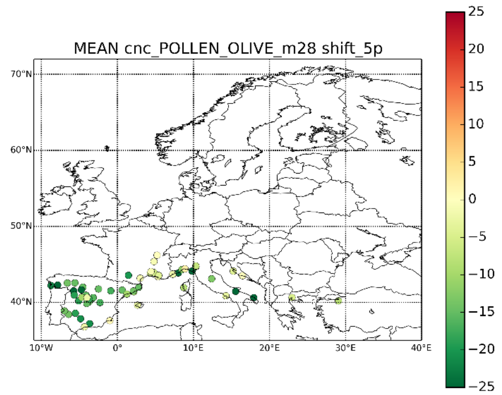

Error in the season start, days

Figure 6. Results of model-measurement comparison for the ensemble mean: correlation coefficient for daily time series, mean bias April-June (pollen m^{-3}), RMSE (pollen m^{-3}), error in the season start (days).

Atmos. Chem. Phys. Discuss., doi:10.5194/acp-2016-1189, 2017
Manuscript under review for journal Atmos. Chem. Phys.
Published: 2 February 2017

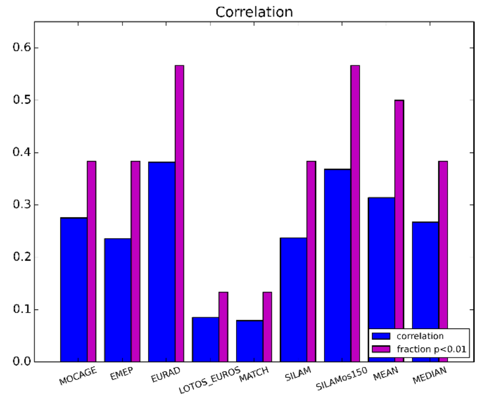

Correlation coefficient and fraction of $p<0.01$

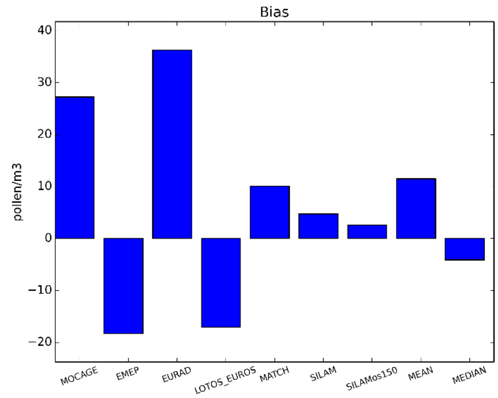

Absolute bias, mean April-June [pollen m^{-3}]

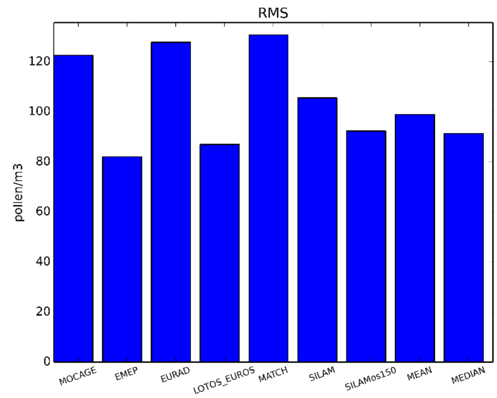

RMSE, [pollen m^{-3}]

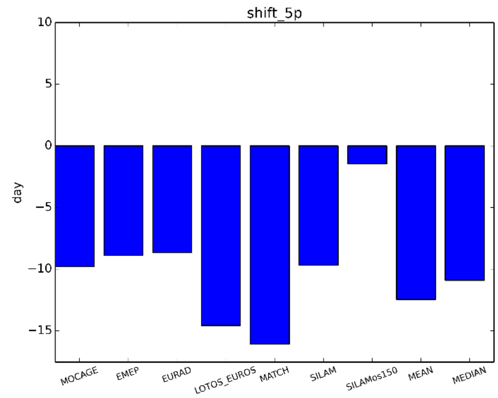

Error in the season start, days

Figure 7. Scores of the individual models, mean over all stations. The same parameters as in **Figure 6**. The sensitivity run SILAMos150 is explained in the discussion section

Atmos. Chem. Phys. Discuss., doi:10.5194/acp-2016-1189, 2017
Manuscript under review for journal Atmos. Chem. Phys.
Published: 2 February 2017

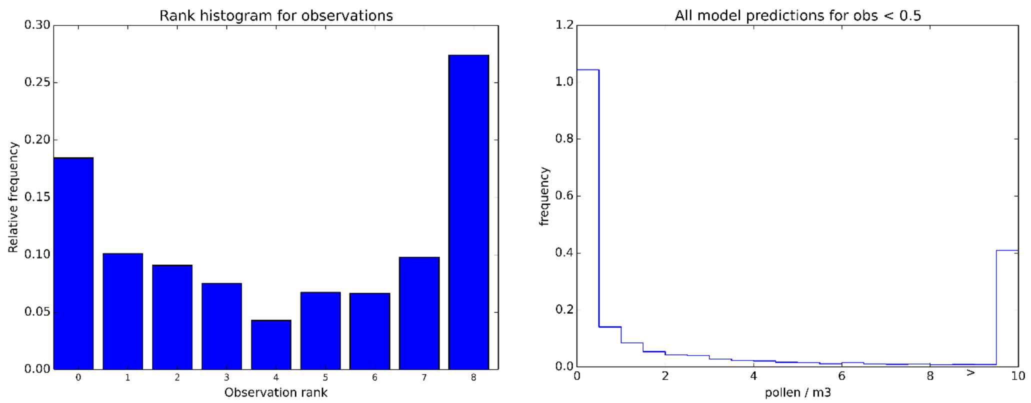

Figure 8. Ensemble characteristics. Left: discrete rank histogram for the constructed ensemble (daily concentration statistics); right: histogram of model predictions when observations were below the detection limit 0.5 pollen m^{-3},

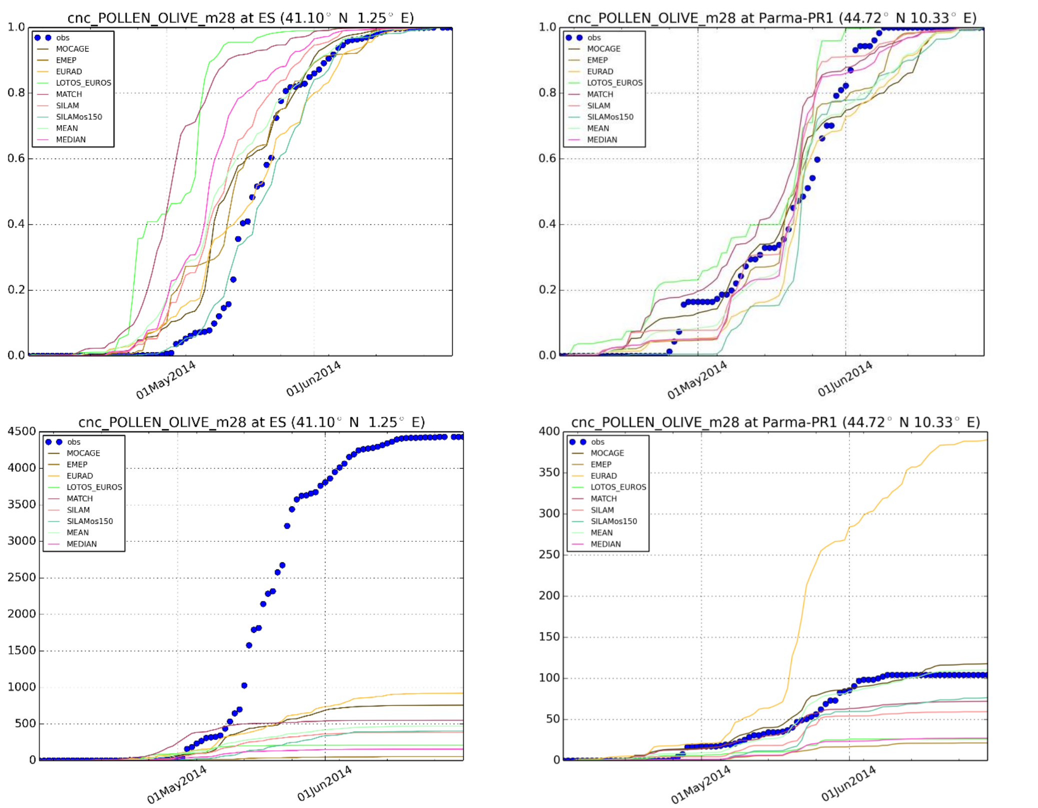

Figure 9. Cumulative time series of olive concentrations at Tarragona (Spain) and Parma (Italy). Upper row: normalized to the seasonal SPI [relative unit], lower: absolute cumulative concentrations [pollen day m^{-3}].

5. Discussion

In this section, we consider the key season parameters and the ability of the presented ensemble to reproduce those (section 5.1), main uncertainties that limit the model scores (section 5.3), and the added value of the multi-model ensembles, including the optimized ensemble (section 5.2).

5.1. Forecast quality: model predictions for the key season parameters

The key date of the pollen season is its start: this very date refers to adaptation measures that need to be taken by allergy sufferers. Predicting this date for olives is a significantly higher challenge than, e.g., for birches: the heat sum has to be accumulated starting from 1 January with the season onset being in mid-April, whereas for birches it is 1 March and mid-March, respectively. As a result, prediction of olive season start strongly depends on the temperature predictions by the weather prediction model. Bias, even if small, over the winter and spring period of almost 4 months can easily lead to a week of an error. As one can see from Figure 7 and Figure 6, there is a systematic bias of all models by about 8 days (too early season). Exception is the SILAMos150 sensitivity run, which used the heat sum threshold 150 degree-days (~10%) higher than the standard level (Figure 2). No other sensitivity runs, including the simulations driven by ERA-Interim fields, showed any significant improvement of this parameter. Importantly, EURAD-IM, which is driven by WRF meteo fields, also showed a similar bias. This calls for an analysis of long-term time series, aiming at refinement of the heat sum formulations and threshold values.

The end of the season showed an intriguing picture: EURAD-IM, despite starting the season as early as all other models, ends it 2 days too late instead of 5 days too early as all other models (see examples for two stations in Figure 9). This indicates that WRF, in late spring, predicts lower temperature than IFS, which leads to longer-than-observed season in the EURAD-IM predictions. A certain daytime cold bias of WRF in late spring and summer has already been noticed at German measurement sites, which corroborates well with this finding. Other models showed correct season length and, due to initial early bias, end it a few days too early. The de-biased run SILAMos150 run shows almost perfect shape and hits both start and end with 1 day accuracy, which supports 250 degree day as a season length parameter.

The most-diverged model predictions are shown for the absolute concentrations (Figure 7). With the mean observed April-June concentration of 35 pollen m^{-3} the range of predictions spans over a factor of four: EURAD-IM and MOCAGE being twice higher and EMEP and LOTOS-EUROS twice lower. Shifting the season by 5 days in the SILAMos150 run also changes the model bias, reflecting differences in the transport patterns and the impact of stronger vertical mixing in later spring. Spatially, the bias is quite homogeneous, except for southern Spain, where heterogeneous pattern is controlled by local conditions at each specific site (Figure 6).

Temporal correlation is generally high in coastal areas (Figure 6) but at or below 0.5 in terrestrial stations of Iberian Peninsula (the main olive plantations). This is primarily caused by the shifted season: the simulations with more accurate season showed the highest correlation among all models with ~60% of sites with significant correlation ($p<0.01$, Figure 7).

5.2. Ensemble added value

Arguably the main uncertainty of the model predictions was caused by the shift of the season start and end – the parameters heavily controlled by temperature, i.e. least affected by transport features of the models. As a result, application of the “simple” ensemble technologies does not lead to a strong improvement. Some effect was still noticed but less significant than in case of birch or traditional AQ forecasting. Therefore, in this section we also consider a possibility of ensemble-based fusion of the observational data with the model predictions. All ensembles were based on operational models, i.e. the SILAMos150 run was not included in either of them.

5.2.1. Mean ensembles: arithmetic average and median

Among the simple means, arithmetic average performed better than the median, largely owing to strong EURAD-IM impact. That model over-estimated the concentrations and introduced a powerful push towards extended season, thus offsetting the early bias of the other models. Since median largely ignored this push, its performance was closer to that of other models. Nevertheless, both mean and median demonstrated low RMSE, median being marginally better.

5.2.2. Fusing the model predictions and observations into an optimized ensemble: gain in the analysis and predictive capacity

Developing further the ensemble technology, we present here the first attempt of fusion of the observational data with the multi-model ensemble for olive pollen.

In the Section 3.1, the Eq. (2) requires three parameters to prescribe: the regularization scaling parameters α and β, and length of the assimilation window T. For the purposes of the current feasibility study, several values for each of the parameters were tested and the robust performance of the ensemble was confirmed with very modest regularization strength and for all considered lengths of the analysis window – from 1 to 15 days. Finally, $\alpha = 0.1$, $\beta = 0.1$, $T = 5\,days$ were selected for the below example as a compromise between the smoothness of the coefficients, regularization strength and the optimization efficiency over the assimilation window.

The optimized ensemble showed (Figure 10, left-hand panel) that each of the 6 models had substantial contribution over certain parts of the period. Over some times, e.g. during the first half of May, only one or two models were used, other coefficients being put to zero, whereas closer to the end of the month, all models were involved. Finally, prior to and after the main season, concentrations were very low and noisy, so the regularization terms of Eq. (2) took over and pushed the weights to a-priori value of 1/6.

The bulk of the improvements came in the first half of the season (Figure 10, middle panel). After the third peak in the middle of May, the effect of assimilation becomes small and the optimization tends to use intercept to meet the mean value, whereas the model predictions become small and essentially uncorrelated with the observations. This corroborates with the observed 8-days shift of the season, which fades out faster in the models than in the observed time series (Figure 9).

There was little reduction of the predictive capacity of the optimized ensemble when going out of assimilation window towards the forecasts. In-essence, only the first peak of concentrations (and RMSE) is better off with shorter forecasts. For the rest of the season (before and after the peak) the 7-day assimilation window led to a robust combination of the models that stayed nearly-optimal over the next five days.

Comparison with other forecasts expectedly shows that the optimized ensemble has significantly better skills than any of the individual models, but also up to 25-30% better than mean and median of the ensemble (Figure 10, middle panel). A stronger competitor was the "persistence forecast" when the next-day(s) concentrations are predicted to be equal the last observed daily value. The one-day persistence appeared to be the best-possible "forecast", which shows at the beginning of May almost twice lower RMSE than the one-day forecast of the optimal ensemble (Figure 10, right-hand panel). However, already two-days persistence forecast had about-same RMSE as the ensemble, and 3- and 4- days predictions were poor.

Atmos. Chem. Phys. Discuss., doi:10.5194/acp-2016-1189, 2017
Manuscript under review for journal Atmos. Chem. Phys.
Published: 2 February 2017

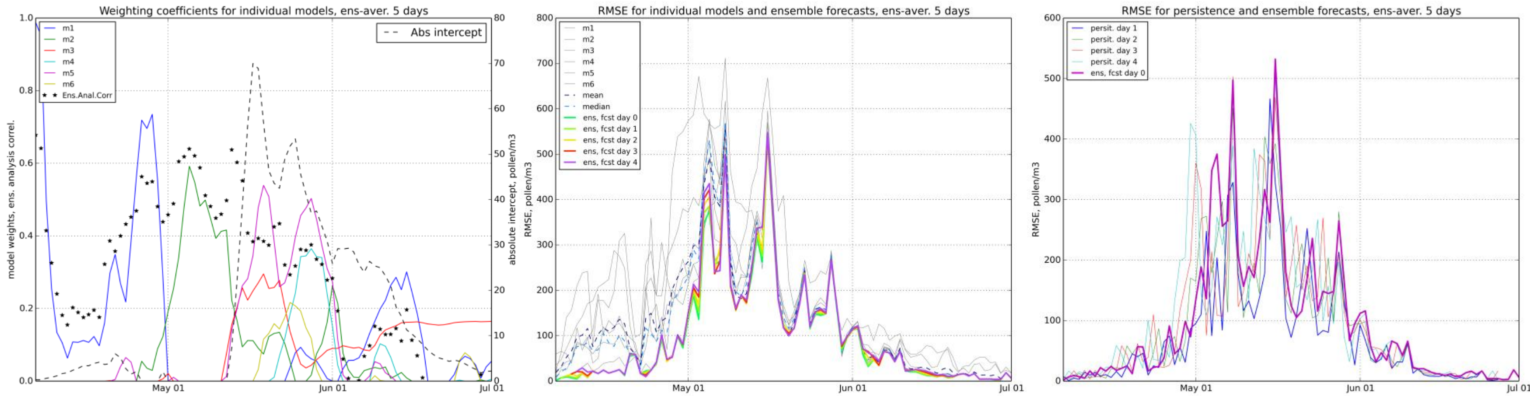

Figure 10. Optimal weights of the individual models and ensemble correlation score over the 5-days-long assimilation window (left panel); RMSE of the of individual models and the optimal ensemble forecasts against those of individual models and simple ensemble means (middle) and against persistence-based forecasts (right-hand panel).

Atmos. Chem. Phys. Discuss., doi:10.5194/acp-2016-1189, 2017
Manuscript under review for journal Atmos. Chem. Phys.
Published: 2 February 2017

Strong performance of the one-day persistence forecast is not surprising and, with the current standards of the pollen observations, has no practical value: the data are always late by more than one day (counting can start only next morning and become available about mid-day). The second problem of the persistence forecast is that it needs actual data, i.e. the scarcity of pollen network then limits its coverage. Thirdly, persistence loses its skills very fast: already day+2 forecast has no superiority to the optimal ensemble, whereas day+3 and +4 persistence-based predictions are useless. Finally, at local scale, state-of-art statistical models can outperform it – see discussion in (Ritenberga et al., 2016).

One should however point out that one-day predicting power of the persistence forecast (or more sophisticated statistical models based on it) can be a strong argument for the future real-time online pollen monitoring, which delay can be as short as one hour (Crouzy et al., 2016; Oteros et al., 2015). Such data have good potential as the next-day predictions for the vicinity of the monitor.

5.3. Sensitivity of the simulations to model and source term parameters

The above-presented results show that arguably the most-significant uncertainty was due to shifting the start and the end of the season. It originated from the long heat sum accumulation (since 1 January), where even a small systematic difference between the meteorology driving the multi-annual fitting simulations and that used for operational forecasts integrates to a significant season shift by late spring. In some areas, resolution of NWP model plays as well: complex terrain in the north of Spain and in Italy requires dense grids to resolve the valleys. Other possible sources of uncertainties might need attention.

To understand the importance of some key parameters, a series of perturbed runs of SILAM was made:

- **os100** and **os150** runs with the season starting threshold increased by 100 and 150 degree days (the **os150** run is referred in the above discussion as SILAMos150)
- **era** run with ERA-Interim meteorological fields, which were used for the source parameters fitting
- series of 3 runs with reduced vertical mixing within the ABL and the free troposphere
- **smlpoll** run with 20 μm size of the pollen grain
- **smlpoll_coarse** run with 20 μm pollen size and coarse computational grid (0.2°×0.2°)

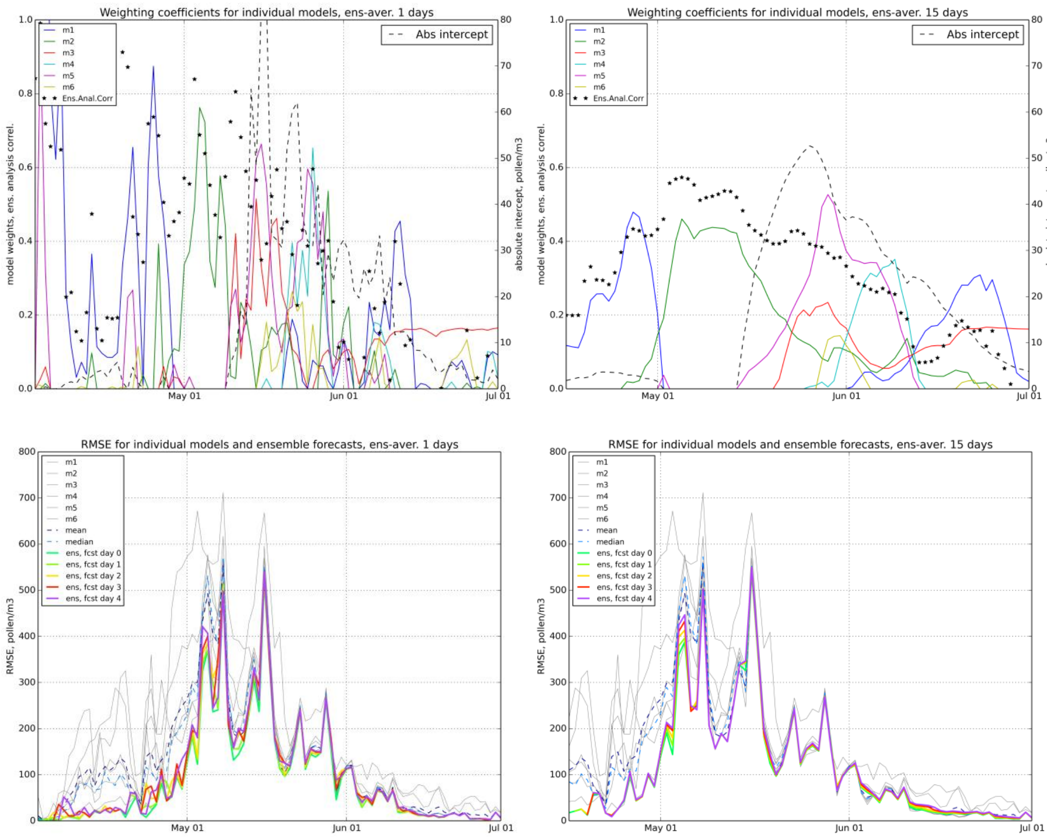

Figure 11. Sensitivity of optimized ensemble to the length of assimilation window. Upper row: optimal weights of the individual models and ensemble score over the 1- (left) and 15- (right) days-long assimilation windows; lower row: RMSE of the of individual models and the optimal ensemble forecasts against those of individual models. Obs. earlier first available date for 1-day-analysis window.

The **era** simulations with ERA-Interim reduced the shift of the season start by 2 days but increased the shift of the end by 3 days, i.e. made the season shorter by 5 days. At the same time, the **os150** run showed that a simple increase of the heat sum threshold by ~10% (150 degree days) essentially eliminates the mean shift – for 2014 – but it remains unclear whether this adjustment is valid for other years.

Variations of the mixing parameterization (perturbing the formula for the K_z eddy diffusivity) did not lead to significant changes: all scores stayed within 10% of the reference SILAM simulations.

Evaluation of the impact of deposition parameterizations was more difficult since they are model-specific. Higher deposition intensity causes both reduction of the transport distance and absolute concentrations. This issue might be behind the low values reported by LOTOS-EUROS and, conversely, high concentrations of EURAD-IM and MOCAGE. Its importance was confirmed by the SILAM sensitivity simulations with smaller pollen size, **smlpoll** and **smlpoll_coarse**. Both runs resulted in more than doubling the mean concentrations but with marginal effect on temporal correlation. They also differed little from each other.

Variations of the fusion parameters showed certain effect. For short averaging window (5 days or less), the variations of weighting coefficients increased and the time series became noisier (Figure 11). On return, the correlation increased almost up to 0.8 – 0.9 for some analysis intervals, though stayed the same for other periods. Also, the one-day forecast RMSE decreased for some days but little difference was found for longer predictions.

6. Summary

An ensemble of 6 CAMS models was run through the olive flowering season of 2014 and compared with observational data of 6 countries of European Aeroallergen Network (EAN).

The simulations showed decent level of reproduction of the short-term phenomena but also demonstrated a shift of the whole season by 8 days (~20% of the overall pollination period). An ad-hoc adjustment of the season-start heat sum threshold by ~10% (150 degree days) resolves the issue and strongly improves the model skills but its validity for other years and meteorological drivers remain unclear.

The ensemble members showed quite diverse pictures demonstrating the substantial variability, especially in areas remote from the main olive plantations. Nevertheless, the observation rank histogram still suggested certain under-statement of the ensemble variability in comparison with the observations.

Simple ensemble treatments, such as arithmetic average and median, resulted in a more robust performance but they did not outrun the best models over significant parts of the season. Arithmetic average turned out to be better than median.

A data-fusion approach, which creates the optimal-ensemble model using the observations over preceding days for optimal combination of the ensemble members, is suggested and evaluated. It

Atmos. Chem. Phys. Discuss., doi:10.5194/acp-2016-1189, 2017
Manuscript under review for journal Atmos. Chem. Phys.
Published: 2 February 2017

was based on an optimal linear combination of the individual ensemble members and showed strong skills, routinely outperforming all individual models and simple ensemble approaches. It also showed strong forecasting skills, which allowed application of the past-time model weighting coefficients over several days in the future. The only approach outperforming this fusion ensemble was the one-day persistence-based forecast, which has no practical value due to the manual pollen observations and limited network density. It can however be used in the future when reliable online pollen observation will become available.

A series of sensitivity simulations highlighted the importance of meteorological driver, especially its temperature representation, and deposition mechanisms. The data fusion procedure was quite robust with regard to analysis interval, still requiring 5-7 days for eliminating the noise in the model weighting coefficients.

7. Acknowledgements

The work was performed within the scope of Copernicus Atmospheric Monitoring Service CAMS, funded by the European Union’s Copernicus Programme. Support by performance-based funding of University of Latvia is also acknowledged. Observational data were provided by national pollen monitoring of Croatia, Greece, France, Italy, Spain, Turkey, members of the European Aeroallergen Network EAN. The olive source term is a joint development of Finnish Meteorological Institute and EAN research teams, created within the scope of the Academy of Finland APTA project. This work contributes to the ICTA 'Unit of Excellence' (MinECo, MDM2015-0552).

The material is published in the name of the European Commission; the Commission is not responsible for any use that may be made of the information/material contained.

8. References

Aguilera, F., Ben Dhiab, A., Msallem, M., Orlandi, F., Bonofiglio, T., Ruiz-Valenzuela, L., Galán, C., Díaz-de la Guardia, C., Giannelli, A., Trigo, M.M., García-Mozo, H., Pérez-, Badia, R., Fornaciari, M., 2015. Airborne-pollen maps for olive-growing areas throughout the Mediterranean region: spatio-temporal interpretation. Aerobiologia (Bologna). 31, 421–434.

Aguilera, F., Ruiz, L., Fornaciari, M., Romano, B., Galán, C., Oteros, J., Ben Dhiab, A., Msallem, M., Orlandi, F., 2013. Heat accumulation period in the Mediterranean region: phenological response of the olive in different climate areas (Spain, Italy and Tunisia). Int. J. Biometeorol.

Atmos. Chem. Phys. Discuss., doi:10.5194/acp-2016-1189, 2017
Manuscript under review for journal Atmos. Chem. Phys.
Published: 2 February 2017

58, 867–876.

Andersen, T.B., 1991. A model to predict the beginning of the pollen season. Grana 30, 269–275. doi:10.1080/00173139109427810

Baklanov, A., Sorensen, J.H., 2001. Parameterisation of radionuclide deposition in atmospheric long-range transport modelling. Phys. Chem. Earth, Parts B 26, 787–799.

Barranco, D., Fernández-Escobar, R., Rallo, L., 2008. El Cultivo del olivo (8ª Ed). Madrid.

Bechtold, P., Bazile, E., Guichard, F., Mascart, P., Richard, E., 2001. A mass-flux convection scheme for regional and global models. Quaterly J. R. Meteorol. Soc. 127, 869–886.

Ben Dhiab, A., Ben Mimoun, M., Oteros, J., Garcia-Mozo, H., Domínguez-Vilches, E., Galán, C., Abichou, M., Msallem, M., 2016. Modeling olive-crop forecasting in Tunisia. Theor. Appl. Climatol. 1–9. doi:10.1007/s00704-015-1726-1

Bott, A., 1989. A positive definite advection scheme obtained by nonlinear renormalization of the advective fluxes. Mon. Weather Rev. 117, 1006–1016.

CEC, 1993. CORINE Land Cover Technical Guide. Luxembourg.

Champeaux, J.L., Masson, V., Chauvin, F., 2005. ECOCLIMAP: a global database of land surface parameters at I km resolution. Meteorol. Appl. 29–32.

Crouzy, B., Stella, M., Konzelmann, T., Calpini, B., Clot, B., 2016. All-optical automatic pollen identification: Towards an operational system. Atmos. Environ. 140, 202–212. doi:10.1016/j.atmosenv.2016.05.062

D'Amato, G., Cecchi, L., Bonini, S., Nunes, C., Annesi-Maesano, I., Behrendt, H., Liccardi, G., Popov, T., van Cauwenberge, P., 2007. Allergenic pollen and pollen allergy in Europe. Allergy 62, 976–90. doi:10.1111/j.1398-9995.2007.01393.x

D'Amato, G., Cecchi, L., Bonini, S., Nunes, C., Annesi-Maesano, I., Behrendt, H., Liccardi, G., Popov, T., van Cauwenberge, P., 2007. Allergenic pollen and pollen allergy in Europe. Allergy 62, 976–990.

Elbern, H., Strunk, A., Schmidt, H., Talagrand, O., 2007. Emission rate and chemical state estimation by 4-dimensional variational inversion. Atmos. Chem. Phys. 7, 3749–3769.

Fernandez-Escobar, R., Benlloch, M., Navarro, C., G.C., M., 1992. The Time of Floral Induction in the Olive. J. Am. Soc. Hortic. Sci. 117, 304–307.

Galan, C., Antunes, C., Brandao, R., Torres, C., Garcia-Mozo, H., Caeiro, E., Ferro, R., Prank, M., Sofiev, M., Albertini, R., Berger, U., Cecchi, L., Celenk, S., Grewling, L., Jackowiak, B., J?ger, S., Kennedy, R., Rantio-Lehtim?ki, A., Reese, G., Sauliene, I., Smith, M., Thibaudon, M., Weber, B., Weichenmeier, I., Pusch, G., Buters, J.T.M., 2013. Airborne olive pollen counts are not representative of exposure to the major olive allergen Ole e 1. Allergy Eur. J. Allergy Clin. Immunol. 68. doi:10.1111/all.12144

Galán, C., García-Mozo, H., Vázquez, L., Ruiz, L., De La Guardia, C.D., Trigo, M., 2005. Heat requirement for the onset of the Olea europaea L. pollen season in several sites in Andalusia and the effect of the expected future climate change. Int. J. Biometeorol. 49, 184–188.

Galán, C., Smith, M., Thibaudon, M., Frenguelli, G., Oteros, J., Gehrig, R., Berger, U., Clot, B., Brandao, R., Group, E.Q.W., 2014. Pollen monitoring: minimum requirements and reproducibility of analysis. Aerobiologia (Bologna). 30, 385–395.

García-mozo, H., Galán, C., Jato, V., Belmonte, J., Díaz, C., Guardia, D., Fernández, D., Aira, M.J., Roure, J.M., Ruiz, L., Trigo, M.M., Domínguez-vilches, E., 2006. Quercus pollen season dynamics in the Iderian Peninsula: response to meteorological parameters and posible consequences of climate change. Ann. Agric. Environ. Med. 209–224.

Garcia-Mozo, H., Yaezel, L., Oteros, J., Galan, C., 2014. Statistical approach to the analysis of olive long-term pollen season trends in southern Spain. Sci. Total Environ. 473–474, 103–109. doi:10.1016/j.scitotenv.2013.11.142

Genikhovich, E., Pavlova, T. V, Kattsov, V.M., 2010. On complexing the ensemble of climate models (In Russian: O komplexirovanii ansamblya klimaticheskih modelej). Proc. Voeikov Main Geophysical Obs. 7, 28–46.

Giorgi, F., Chameides, W.L., 1986. Rainout lifetimes of highly soluble aerosols and gases as inferred from simulations with a general circulation model. J. Geophys. Res. 91, 14367–14376.

Gioulekas, D., Papakosta, D., Damialis, A., Spieksma, F.T.M., Giouleka, P., Patakas, D., 2004. Allergenic pollen records (15 years) and sensitization in patients with respiratory allergy in Thessaloniki , Greece. Allergy 174–184.

Gómez, J.A., Infante-Amate, J., González de Molina, M., Vanwalleghem, T., Taguas, E.V., Lorite, I., 2014. Olive Cultivation, its Impact on Soil Erosion and its Progression into Yield Impacts in Southern Spain in the Past as a Key to a Future of Increasing Climate Uncertainty. Agriculture 4, 170–198. doi:10.3390/agriculture4020170

Hass, H., Jakobs, H.J., Memmesheimer, M., 1995. Analysis of a regional model (EURAD) near surface gas concentration predictions using observations from networks. Meteorol. Atmos. Phys. 57, 173–200.

Hirst, J.M., 1952. An automatic volumetric spore trap. Ann. Appl. Biol. 39, 257–265. doi:10.1111/j.1744-7348.1952.tb00904.x

Holtslag, A.A.., Nieuwstadt, F.T.M., 1986. Scaling the atmospheric boundary layer. Bound. Layer Meteorol. 36, 201–209.

Johansson, L., Epitropou, V., Karatzas, K., Karppinen, A., Wanner, L., Vrochidis, S., Bassoukos, A., Kukkonen, J., Kompatsiaris, I., 2015. Fusion of meteorological and air quality data extracted from the web for personalized environmental information services. Environ. Model. Softw. 64, 143–155. doi:10.1016/j.envsoft.2014.11.021

Josse, B., Simon, P., Peuch, V., 2004. Radon global simulations with the multiscale chemistry and transport model MOCAGE. Tellus B 56, 339–356.

Jäger, S., Mandroli, P., Spieksma, F., Emberlin, J., Hjelmroos, M., Rantio-Lehtimaki, A., Al, E., 1995. News. Aerobiologia (Bologna). 11, 69–70.

Kalyoncu, A., Qoplii, L., Selguk, Z., Emri, A., Kolagan, B., Kocabas, A., 1995. Survey of the allergic status of patients with bronchial asthma in Turkey : a multicenter study. Allergy 50, 451–456.

Kouznetsov, R., Sofiev, M., 2012. A methodology for evaluation of vertical dispersion and dry deposition of atmospheric aerosols. J. Geophys. Res. 117. doi:doi:10.1029/2011JD016366

Kukkonen, J., Olsson, T., Schultz, D.M., Baklanov, a., Klein, T., Miranda, a. I., Monteiro, a., Hirtl, M., Tarvainen, V., Boy, M., Peuch, V.-H., Poupkou, a., Kioutsioukis, I., Finardi, S., Sofiev, M., Sokhi, R., Lehtinen, K.E.J., Karatzas, K., San José, R., Astitha, M., Kallos, G., Schaap, M., Reimer, E., Jakobs, H., Eben, K., 2012. A review of operational, regional-scale, chemical weather forecasting models in Europe. Atmos. Chem. Phys. 12, 1–87.

Atmos. Chem. Phys. Discuss., doi:10.5194/acp-2016-1189, 2017
Manuscript under review for journal Atmos. Chem. Phys.
Published: 2 February 2017

Atmospheric Chemistry and Physics Discussions

doi:10.5194/acp-12-1-2012

Langner, J., Bergström, R., Pleijel, K., 1998. European scale modeling of sulphur, oxidized nitrogen and photochemical oxidants. Model dependent development av evaluation for the 1994 growing season. Norkoping.

Linkosalo, T., Ranta, H., Oksanen, A., Siljamo, P., Luomajoki, A., Kukkonen, J., Sofiev, M., 2010. A double-threshold temperature sum model for predicting the flowering duration and relative intensity of Betula pendula and B. pubescens. Agric. For. Meteorol. 6–11. doi:10.1016/j.agrformet.2010.08.007

Louis, J.-F., 1979. A parametric model of vertical eddy fluxes in the atmosphere. Bound. Layer Meteorol. 17, 187–202.

Loureiro, G., Rabaca, M.A., Blanco, B., Andrade, S., Chieira, C., Pereira, C., 2005. Aeroallergens' sensitization in an allergic paediatric population of Cova da Beira, Portugal. Allergol. Immunopathol. (Madr). 33, 192–198.

Mandrioli, P., Comtois, P., V., L. (Eds.), 1998. Methods in Aerobiology. Pitagora Editrice, Bologna.

Marécal, V., Peuch, V.-H., Andersson, C., Andersson, S., Arteta, J., Beekmann, M., Benedictow, A., Bergström, R., Bessagnet, B., Cansado, A., Chéroux, F., Colette, A., Coman, A., Curier, R.L., Denier van der Gon, H. a. C., Drouin, A., Elbern, H., Emili, E., Engelen, R.J., Eskes, H.J., Foret, G., Friese, E., Gauss, M., Giannaros, C., Guth, J., Joly, M., Jaumouillé, E., Josse, B., Kadygrov, N., Kaiser, J.W., Krajsek, K., Kuenen, J., Kumar, U., Liora, N., Lopez, E., Malherbe, L., Martinez, I., Melas, D., Meleux, F., Menut, L., Moinat, P., Morales, T., Parmentier, J., Piacentini, A., Plu, M., Poupkou, A., Queguiner, S., Robertson, L., Rouïl, L., Schaap, M., Segers, A., Sofiev, M., Thomas, M., Timmermans, R., Valdebenito, Á., van Velthoven, P., van Versendaal, R., Vira, J., Ung, A., 2015. A regional air quality forecasting system over Europe: the MACC-II daily ensemble production. Geosci. Model Dev. 8, 2777–2813. doi:10.5194/gmd-8-2777-2015

Martet, M., Peuch, V.-H., Laurent, B., B., M., Bergametti, G., 2009. Evaluation of long-range transport and deposition of desert dust with the CTM Mocage. Tellus B 61, 449–463.

Masson, V., Champelaux, J.-L., Chauvin, F., Meriguet, C., Lacaze, R., 2003. A Global Database of Land Surface Parameters at 1-km Resolution in Meteorological and Climate Models. J. Clim. 16, 1261–1282.

Memmesheimer, M., Friese, E., Ebel, A., Jakobs, H.J., Feldmann, H., Kessler, C., Piekorz, G., 2004. Long-term simulations of particulate matter in Europe on different scales using sequential nesting of a regional model. Int. J. Environ. Pollut. 22, 108–132.

Moriondo, M., Orlandini, S. De, P., N., Mandrioli, P., 2001. Effect of agrometeorological parameters on the phenology of pollen emission and production of olive trees (Olea europea L.). Aerobiologia (Bologna). 225–232. doi:doi:10.1023/A:1011893411266

Negrini, A.C., Ariano, R., Delbono, G., Ebbli, A., Quaglia, A., Arobba, D., Allergologia, A., Paolo, O.S., Ligure, P., Sv, I.-P.L., 1992. Incidence of sensitisation to the pollens of Urticaceae (Parietaria), Poaceae and Oleaceae (Olea europaea) and pollen rain in Liguria (Italy). Aerobiologia (Bologna). 8, 355–358.

Orlandi, F., Romano, B., Fornaciari, M., 2005a. Effective pollination period estimation in olive (Olea europaea L.): A pollen monitoring application. Sci. Hortic. (Amsterdam). 313–318. doi:doi:10.1016/j.scienta.2005.01.012

Atmos. Chem. Phys. Discuss., doi:10.5194/acp-2016-1189, 2017
Manuscript under review for journal Atmos. Chem. Phys.
Published: 2 February 2017

Orlandi, F., Vazquez, L.M., Ruga, L., Bonofiglio, T., Fornaciari, M., Garcia-Mozo, H., Domínguez, E., Romano, B., Galan, C., 2005b. Bioclimatic requirements for olive flowering in two mediterranean regions located at the same latitude (Andalucia, Spain, and Sicily, Italy). Ann. Agric. Environ. Med. 47–52.

Oteros, J., Garcia-Mozo, H., Vazquez, L., Mestre, A., Dominguez-Vilches, E., Galan, C., 2013. Modelling olive phenological response to weather and topography. Agric. Ecosyst. Environ. 179, 62–68.

Oteros, J., García-Mozo, H., Alcázar, P., Belmonte, J., Bermejo, D., Boi, M., Cariñanos, P., Díaz de la Guardia, C., Fernández-González, D., González-Minero, F., Gutiérrez-Bustillo, A.M., Moreno-Grau, S., Pérez-Badia, R., Rodríguez-Rajo, F.J., Ruíz-Valenzuela, L., Suárez-Pérez, J., Trigo, M.M., Domínguez-Vilches, E., Galán, C., 2015. A new method for determining the sources of airborne particles. J. Environ. Manage. 155, 212–218.

Oteros, J., Orlandi, F., Aguilera, F., Ben, A., Bonofiglio, T., 2014. Better prediction of Mediterranean olive production using pollen-based models. Agron. Sustain. Dev. 34, 685–694. doi:10.1007/s13593-013-0198-x

Oteros, J., Pusch, G., Weichenmeier, I., Heimann, U., Möller, R., Röseler, S., Traidl-Hoffmann, C., Schmidt-Weber, C., Buters, J.T.M., 2015. Automatic and online pollen monitoring. Int. Arch. Allergy Immunol. 167, 158–166. doi:10.1159/000436968

Petroff, A., Zhang, L., 2010. Development and application of a size-resolved particle dry deposition scheme for application in aerosol transport models. Geosci. Model Dev. 3, 753–769. doi:doi: 10.5197/gmd-3-753-2010

Potempski, S., Galmarini, S., 2009. and Physics Est modus in rebus : analytical properties of multi-model ensembles. Atmos. Chem. Phys. 9, 9471–9489.

Prank, M., Chapman, D.S., Bullock, J.M., Belmonte, J., Berger, U., Dahl, A., Jäger, S., Kovtunenko, I., Magyar, D., Niemelä, S., Rantio-Lehtimäki, A., Rodinkova, V., Sauliene, I., Severova, E., Sikoparija, B., Sofiev, M., 2013. An operational model for forecasting ragweed pollen release and dispersion in Europe. Agric. For. Meteorol. 182–183, 43–53. doi:10.1016/j.agrformet.2013.08.003

Ritenberga, O., Sofiev, M., Kirillova, V., Kalnina, L., Genikhovich, E., 2016. Statistical modelling of non-stationary processes of atmospheric pollution from natural sources : example of birch pollen. Agric. For. Meteorol. 226–227, 96–107. doi:10.1016/j.agrformet.2016.05.016

Robertson, L., Langner, J., 1999. An Eulerian Limited-Area Atmospheric Transport Model. J. Appl. Meteorol. 38, 190–210.

Rojo, J., Pérez-Badia, R., 2015. Spatiotemporal analysis of olive flowering using geostatistical techniques. Sci. Total Environ. 505, 860–869.

Sánchez-Mesa, J.A., Serrano, P., Cariñanos, P., Prieto-Baena, J.., Moreno, C., Guerra, F., Galan, C., 2005. Pollen allergy in Cordoba city: frequency of sensitization and relation with antihistamine sales. J. Investig. Allergol. Clin. Immunol. 15, 50–56.

Schaap, M., Timmermans, R. M. A., Roemer, M., Boersen, G.A.C., Builtjes, P.J.H., Sauter, F.J., Velders, G.J.M., Beck, J.P., 2008. The LOTOS-EUROS model: Description, validation and latest developments. Int. J. Environ. Pollut. 32, 270–290.

Scott, B.C., 1979. Parameterization of sulphate removal by precipitation. J. Appl. Meteorol. 17, 11275–11389.

Atmos. Chem. Phys. Discuss., doi:10.5194/acp-2016-1189, 2017
Manuscript under review for journal Atmos. Chem. Phys.
Published: 2 February 2017

Seinfeld, J.H., Pandis, S.N., 1998. Atmospheric Chemistry and Physics, 1st ed. Wiley, New Yeork.

Siljamo, P., Sofiev, M., Ranta, H., Linkosalo, T., Kubin, E., Ahas, R., Genikhovich, E., Jatczak, K., Jato, V., Nekovar, J., Minin, A., Severova, E., Shalabova, V., 2008. Representativeness of point-wise phenological Betula data collected in different parts of Europe. Glob. Ecol. Biogeogr. 17, 489–502. doi:10.1111/j.1466-8238.2008.00383.x

Simpson, D., Benedictow, a., Berge, H., Bergström, R., Emberson, L.D., Fagerli, H., Flechard, C.R., Hayman, G.D., Gauss, M., Jonson, J.E., Jenkin, M.E., Nyíri, a., Richter, C., Semeena, V.S., Tsyro, S., Tuovinen, J.-P., Valdebenito, Á., Wind, P., 2012. The EMEP MSC-W chemical transport model – technical description. Atmos. Chem. Phys. 12, 7825–7865. doi:10.5194/acp-12-7825-2012

Simpson, D., Fagerli, H., Jonson, J.E., Tsyro, S., Wind, P., Tuovinen, J.-P., 2003. Transboundary Acidification, Eutrophication and Ground Level Ozone in Europe, Part 1: Unified EMEP Model Description. EMEP Report 1/2003. Oslo.

Sofiev, M., 2016. On impact of transport conditions on variability of the seasonal pollen index. Aerobiologia (Bologna). doi:10.1007/s10453-016-9459-x

Sofiev, M., 2002. Extended resistance analogy for construction of the vertical diffusion scheme for dispersion models. J. Geophys. Res. 107, ACH 10-1–ACH 10-8. doi:10.1029/2001JD001233

Sofiev, M., Berger, U., Prank, M., Vira, J., Arteta, J., Belmonte, J., Bergmann, K.C., Charoux, F., Elbern, H., Friese, E., Galan, C., Gehrig, R., Khvorostyanov, D., Kranenburg, R., Kumar, U., Marecal, V., Meleux, F., Menut, L., Pessi, A.-M., Robertson, L., Ritenberga, O., Rodinkova, V., Saarto, A., Segers, A., Severova, E., Sauliene, I., Siljamo, P., Steensen, B.M., Teinemaa, E., Thibaudon, M., Peuch, V.-H., 2015. MACC regional multi-model ensemble simulations of birch pollen dispersion in Europe. Atmos. Chem. Phys. 15, 8115–8130. doi:10.5194/acp-15-8115-2015

Sofiev, M., Siljamo, P., Ranta, H., Linkosalo, T., Jaeger, S., Rasmussen, A., Rantio-Lehtimaki, A., Severova, E., Kukkonen, J., 2012. A numerical model of birch pollen emission and dispersion in the atmosphere. Description of the emission module. Int. J. Biometeorol. 57, 54–58. doi:10.1007/s00484-012-0532-z

Sofiev, M., Siljamo, P., Valkama, I., Ilvonen, M., Kukkonen, J., 2006. A dispersion modelling system SILAM and its evaluation against ETEX data. Atmos. Environ. 40, 674–685. doi:10.1016/j.atmosenv.2005.09.069

Sofiev, M., Vira, J., Kouznetsov, R., Prank, M., Soares, J., Genikhovich, E., 2015. Construction of the SILAM Eulerian atmospheric dispersion model based on the advection algorithm of Michael Galperin. Geosci. Model Dev. 8. doi:10.5194/gmd-8-3497-2015

Spano, D., Cesaraccio, C., Duce, P., Snyder, R.L., 1999. Phenological stages of natural species and their use as climate indicators. Int. J. Biometeorol. 124–133. doi:doi:10.1007/s004840050095

Spieksma, F.T.., 1990. Pollinosis in Europe: New observations and developments. Rev. Palaeobot. Palynol. 64, 35–40.

Venkatram, A., 1978. Estimating the convective velocity scale for diffusion applications. Bound. Layer Meteorol. 15, 447–452.

Walcek, C.J., Aleksic, N.M., 1998. A simple but accurate mass conservative, peak-preserving, mixing ratio bounded advection algorithm with FORTRAN code. Atmos. Environ. 32, 3863–3880. doi:10.1016/S1352-2310(98)00099-5

Atmos. Chem. Phys. Discuss., doi:10.5194/acp-2016-1189, 2017
Manuscript under review for journal Atmos. Chem. Phys.
Published: 2 February 2017

Williamson, D.L., Rasch, P., 1989. Two-Dimensional Semi-Lagrangian Transport with Shape-Preserving Interpolation. Am. Meteorol. Soc. 117, 102–129.

Zhang, L., Gong, S., Padro, J., Barrie, L., 2001. A size-segregated particle dry deposition scheme for an atmospheric aerosol module. Atmos. Environ. 35, 549–560.